

Nature and stability of the (100) Si/La Al O 3 interface probed by paramagnetic defects

A. Stesmans, K. Clémer, V. V. Afanas'ev, L. F. Edge, and D. G. Schlom

Citation: [Applied Physics Letters](#) **89**, 112121 (2006); doi: 10.1063/1.2219334

View online: <http://dx.doi.org/10.1063/1.2219334>

View Table of Contents: <http://scitation.aip.org/content/aip/journal/apl/89/11?ver=pdfcov>

Published by the [AIP Publishing](#)

Articles you may be interested in

[Inherent point defects at the thermal higher-Miller index \(211\)Si/SiO₂ interface](#)

Appl. Phys. Lett. **105**, 262101 (2014); 10.1063/1.4904413

[Paramagnetic point defects at Si O 2 /nanocrystalline Si interfaces](#)

Appl. Phys. Lett. **93**, 023123 (2008); 10.1063/1.2952276

[Paramagnetic point defects in \(100 \) Si/La Al O 3 structures: Nature and stability of the interface](#)

J. Appl. Phys. **102**, 034516 (2007); 10.1063/1.2749423

[Si dangling-bond-type defects at the interface of \(100\)Si with ultrathin layers of SiO_x, Al₂O₃, and ZrO₂](#)

Appl. Phys. Lett. **80**, 1957 (2002); 10.1063/1.1448169

[Paramagnetic defects at the interface of ultrathin oxides grown under vacuum ultraviolet photon excitation on \(111\) and \(100\) Si](#)

Appl. Phys. Lett. **77**, 1469 (2000); 10.1063/1.1289265

An advertisement for Oxford Instruments' Asylum Research AFM. The background is dark blue with a light blue gradient. On the left, there is a black mobile phone and a white desktop computer. In the center, there is a white AFM instrument. Text on the left says 'You don't still use this cell phone or this computer'. Text in the center asks 'Why are you still using an AFM designed in the 80's?'. Text on the right says 'It is time to upgrade your AFM', 'Minimum \$20,000 trade-in discount for purchases before August 31st', and 'Asylum Research is today's technology leader in AFM'. At the bottom right, there is the Oxford Instruments logo and the tagline 'The Business of Science®'. The email address 'dropmyoldAFM@oxinst.com' is also present.

You don't still use this cell phone or this computer

Why are you still using an AFM designed in the 80's?

It is time to upgrade your AFM

Minimum \$20,000 trade-in discount for purchases before August 31st

Asylum Research is today's technology leader in AFM

dropmyoldAFM@oxinst.com

OXFORD
INSTRUMENTS
The Business of Science®

Nature and stability of the (100)Si/LaAlO₃ interface probed by paramagnetic defects

A. Stesmans,^{a)} K. Clémer, and V. V. Afanas'ev
Department of Physics, University of Leuven, 3001 Leuven, Belgium

L. F. Edge and D. G. Schlom
*Department of Materials Science and Engineering, Pennsylvania State University,
 University Park, Pennsylvania 16802-5005*

(Received 11 April 2006; accepted 22 May 2006; published online 14 September 2006)

Electron spin resonance analysis of (100)Si/LaAlO₃ structures reveals the absence of a Si/SiO₂-type interface in terms of archetypal Si-dangling bond-type Si/SiO₂ interface defects (P_{b0}, P_{b1}). With no P_b -type defects observed, this state is found to persist during subsequent annealing (5% O₂+N₂ ambient) up to $T_{\text{an}} \sim 800$ °C, indicating a thermally stable and abrupt Si/LaAlO₃ interface. In the range $T_{\text{an}} \sim 800$ – 860 °C, however, a Si/SiO₂-type interface starts forming as evidenced by the appearance of P_{b0} defects and, with some delay in T_{an} , the EX center (a SiO₂ associated defect) attesting to significant structural/compositional modification. The peaking of the defect density versus T_{an} curves indicates that the interlayer with SiO_x nature breaks up upon annealing at $T_{\text{an}} \geq 930$ °C, possibly related to crystallization and silicate formation. No LaAlO₃-specific point defects could be detected. © 2006 American Institute of Physics. [DOI: 10.1063/1.2219334]

With the relentless scaling of Si/SiO₂-based complementary metal oxide semiconductor (CMOS) transistors, one targeted revolutionary impact concerns the replacement of the conventional SiO₂ gate dielectric by one of higher dielectric constant κ .¹ Intensely investigated candidates are metal oxides in their simplest form such as Al₂O₃, HfO₂, La₂O₃, ZrO₂, and others,^{2,3} as well as more complicated varieties. Currently, the leading contenders are Hf-based insulators, with the main focus on nitrated Hf silicate (HfSi_xO_yN_z).^{1,4} Special attention has been paid to the Si/high- κ dielectrics interface, since its quality fundamentally influences device performance. Typically, the process used to deposit metal oxides directly on Si results in the formation of a SiO₂ interfacial layer, as revealed by numerous topographic/imaging techniques, such as medium-energy ion scattering (MEIS), high-resolution transmission electron microscopy (HRTEM), and x-ray photoelectron spectroscopy (XPS).⁵

On the atomic scale, this has been prominently demonstrated initially by *K*-band electron spin resonance (ESR) work⁶ on stacks of (100)Si with nanometer-thick layers of Al₂O₃ and ZrO₂ grown by the atomic layer chemical vapor deposition (CVD) method, which revealed the presence at the Si/dielectric interface of Si-dangling bond-type point defects (P_{b0}, P_{b1})—the archetypal defects for the (100)Si/SiO₂ (SiO_xN_y) interface. It has since been confirmed by various independent ESR studies.⁷ The P_b -type defects are the dominant class of interface traps invariably introduced at the Si/SiO₂ interface as a result of lattice mismatch.^{8–10} Their presence in Si/high- κ structures would thus convincingly demonstrate the presence of a SiO_x-type interlayer. So far three types of Si-dangling bond-type interface defects have been established by ESR. All three variants, P_b in (111) Si/SiO₂ and P_{b0} and P_{b1} in (100)Si/SiO₂, were shown to be trivalent Si centers^{9–12} and naturally occurring, for standard

oxidation temperatures T_{ox} (800–960 °C), in areal densities of¹⁰ $[P_b] \sim 5 \times 10^{12}$ cm⁻² and⁶ $[P_{b0}], [P_{b1}] \sim 1 \times 10^{12}$ cm⁻². The chemically identical P_b and P_{b0} were established as dominant detrimental interface traps.

Despite the superb electronic quality of the Si/SiO₂ interface, the presence of an interfacial SiO_x layer in Si/high- κ structures is not desirable in view of minimizing the net equivalent Si-oxide thickness (EOT). Park and Ishiwara deposited the first LaAlO₃ thin films ($\kappa=20$ – 27) on (100) Si using molecular-beam deposition (MBD).¹³ Later, Edge *et al.* showed through an intensive study combining infrared absorption, Auger electron spectroscopy, MEIS, HRTEM, and XPS that it was possible for as-deposited amorphous (a) LaAlO₃ films on Si grown by MBD to have <0.2 Å of SiO₂ at the LaAlO₃/Si interface.¹⁴ This remarkable result allows the elimination of the SiO_x interlayer, but at the same time raises the question regarding quality, both in atomic and electrical terms, of the abrupt Si/LaAlO₃ interface. In a recent paper,¹⁵ Sivasubramani *et al.* investigated these *a*-LaAlO₃/Si entities as a function of postdeposition rapid thermal annealing (RTA) for 20 s in flowing N₂. They observed a change in the structure of LaAlO₃ from amorphous to polycrystalline after a 935 °C RTA and La and Al penetration into the Si after RTA at temperatures ≥ 950 °C.

As, to the best of our knowledge, abrupt Si/metal oxide interfaces have not yet been characterized at the atomic level, it is of interest to gain more in depth information on the true interfacial nature of Si/LaAlO₃ structures and the consequences of postdeposition anneals (PDAs). The present work provides structural information on the atomic scale by monitoring paramagnetic point defects in (100)Si/LaAlO₃ structures. We demonstrate, through the occurrence/absence of interface specific (P_{b0}, P_{b1}) and/or interlayer associated (EX) point defects, the appearance, additional growth, and modification of a SiO_x interlayer at $T_{\text{an}} \geq 860$ °C.

The amorphous (30–60 nm thick) LaAlO₃ thin films were deposited by MBD on *p*-type (100)Si[(3–6)

^{a)}Electronic mail: andre.stesmans@fys.kuleuven.

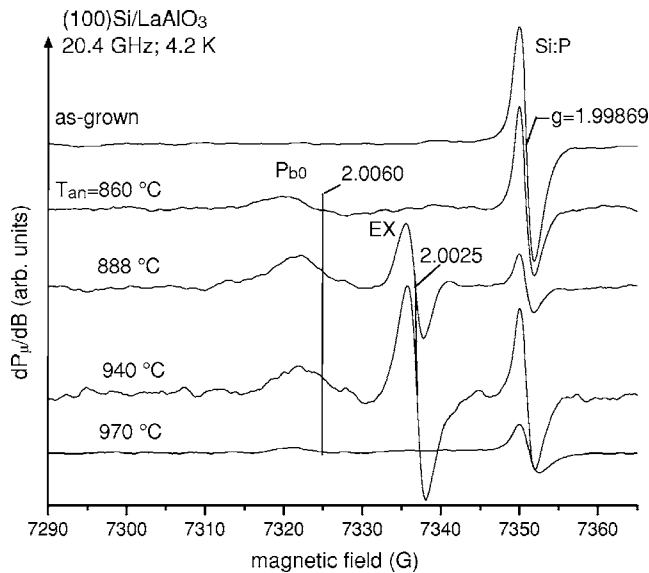


FIG. 1. Derivative-absorption K -band ESR spectra measured at 4.2 K for \mathbf{B} perpendicular to the interface of (100)Si/LaAlO₃ structures subjected to different PDAs in N₂+5% O₂ (10 min). Spectral heights were normalized to equal marker intensity and sample area. The applied modulation field amplitude B_m was 0.6 G and incident microwave power $P_\mu \sim 2.5$ nW. The signal at $g=1.99869$ stems from the comounted Si:P marker sample.

$\times 10^{15}$ B/cm³] at room temperature using elemental sources.¹⁷ This deposition process has been shown to produce stoichiometric amorphous LaAlO₃ thin films with an abrupt LaAlO₃/Si interface.¹⁴ From these wafers, ESR slices of 2×9 mm² main area were cut with the 9 mm edge along a $\langle 0\bar{1}1 \rangle$ direction. Cutting damage was removed through selective chemical etching. The thermal stability of the deposited LaAlO₃ layers and interfaces was analyzed by subjecting samples to ~ 10 min PDA at desired temperatures between 630 and 1000 °C generally in a 1 atm N₂+5% O₂ (99.995%) ambient. Several sets of samples were used for the various thermal steps. As an additional test related to potential ESR activation/maximalization of paramagnetic defects some samples were subjected for 10 min to 10.02 eV vacuum UV photons ($\sim 5 \times 10^{14}$ cm⁻² s⁻¹) or short positive corona charging (3 μ A for 10 s). Conventional cw slow-passage K -band ESR measurements were carried out⁶ at 4.2 K for the applied magnetic field \mathbf{B} rotating in the $(0\bar{1}1)$ Si plane with respect to the $[100]$ interface normal \mathbf{n} .

Figure 1 shows an overview of ESR spectra, observed with $\mathbf{B} \parallel \mathbf{n}$ on the as-deposited (100)Si/LaAlO₃ structure and after different PDA steps. Within spectral accuracy, no ESR active defects could be observed on the as-deposited samples; the spectra remained unchanged for annealing up to $T_{\text{an}} \leq 800$ °C. Upon annealing in the temperature range $T_{\text{an}} \sim 860$ –970 °C, however, a resonance signal is observed at zero crossing $g=2.0060 \pm 0.0001$ with peak-to-peak width $\Delta B_{\text{pp}} = (7 \pm 1)$ G, exhibiting distinct angular anisotropy. To trace the signal's origin, a g map was composed for \mathbf{B} rotating in the $(0\bar{1}1)$ plane. The data could be well fitted by an axial symmetric system with principal g values $g_{\parallel} = 2.0017 \pm 0.0001$ and $g_{\perp} = 2.0082 \pm 0.0001$. This result matches the g pattern of the P_{b0} defect in standard thin SiO₂/Si systems,¹² leaving little doubt about the signal's origin. It appears that the (100)Si/LaAlO₃ interface has become Si/SiO_{2(x)} type, evidencing that a SiO_x-type interlayer has

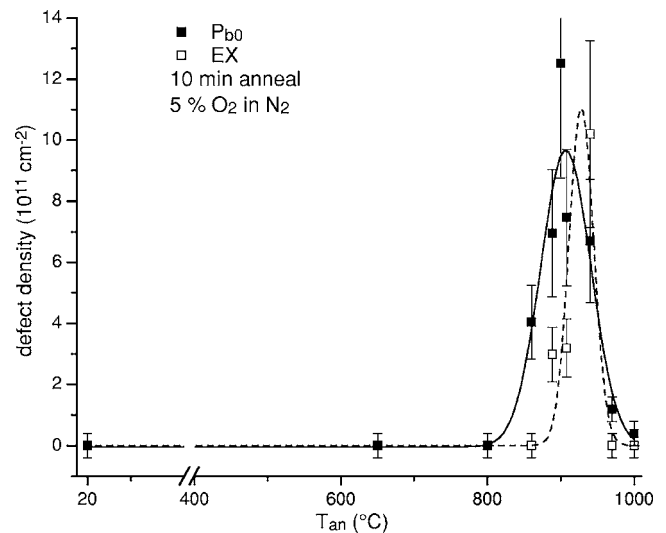


FIG. 2. Overview of the defect densities (inferred through double numerical integration) in (100)Si/LaAlO₃ entities as a function of isochronal PDA in N₂+5% O₂ (10 min) for P_{b0} and EX centers, represented by the closed and open symbols, respectively. The solid and dashed lines are Gaussian curves, merely meant to guide the eye in exposing the peaking in defect generation and the somewhat lagging behind (~ 30 °C) of EX production vis-à-vis P_{b0} . Data points at zero defect density mean that no signal could be detected.

formed. As can be seen from Fig. 1, another signal is observed after annealing in the range $T_{\text{an}} \sim 888$ –940 °C at $g = 2.0025 \pm 0.0001$. This could be identified as the EX signal from the observed accompanying hyperfine doublet (16.4 G splitting) centered around this g value, typically observed for this defect,¹⁶ The EX defect is a SiO₂ associated center, which is well known from studies of Si/SiO₂ structures.¹⁷

No LaAlO₃-specific point defects could be observed either on the as-deposited samples or after PDA nor after additional corona or vuv treatment.

The main PDA results (5% O₂+N₂) are compiled in Fig. 2 showing the density of observed defects as a function of PDA temperature. Several aspects are worth noting. (1) No ESR signals, in particular, no P_b -type defects, could be observed in the as-deposited Si/LaAlO₃ structure. On the basis of the latter criterion it evidences, with atomic level sensitivity, that there is no SiO_x-type interlayer present or that this interlayer is at least substantially thinner than¹⁸ 3 Å—an abrupt interface—which is in good agreement with our previous results.¹⁴ This is in sharp contrast with other stacks of (100) Si with high- κ layers, such as Al₂O₃, HfO₂, and ZrO₂, where the presence of such an interlayer appeared inevitable, even in the as-deposited state, which was revealed by ESR.^{6,7} The abrupt interface remains unaltered even during subsequent annealing up to $T_{\text{an}} \leq 800$ °C, indicating that the interface is thermally stable. (2) After annealing at $T_{\text{an}} \sim 860$ °C a SiO_x-type interlayer has formed, as evidenced by the observation of P_{b0} defects. (3) Upon annealing at a slightly higher temperature $T_{\text{an}} \sim 888$ °C, the SiO₂-associated EX defect appears, so delayed over ~ 30 °C in terms of T_{an} . This observation corroborates the presence of a SiO_x-type interlayer and also indicates an additional growth of the interlayer. The defect was not observed in the sample annealed at $T_{\text{an}} \sim 860$ °C even though the presence of a SiO_x-type interlayer in this sample is signaled by the observation of P_{b0} defects. It suggests that a minimal thickness of the SiO_x interlayer is needed for (ESR) detectable formation of EX defects, at least more substantial than required for effective Si/SiO_x-interface

formation. The interlayer thickness, however, is unknown. In broader context, it is interesting to note that the generation of *EX* centers upon annealing at elevated temperatures in oxygen-containing ambients appears symptomatic for stacks of high- κ metal oxide layers on Si.¹⁹

Prominently, the defect density versus T_{an} curves (Fig. 2) show a peaked behavior, simulated by Gaussian curves. The maximum P_{b0} density (P_{b0}) $\sim (1.3 \pm 0.3) \times 10^{12} \text{ cm}^{-2}$ is obtained at $T_{\text{an}} = 900 \text{ }^\circ\text{C}$ while the maximum *EX* density [*EX*] $\sim (1.0 \pm 0.3) \times 10^{12} \text{ cm}^{-2}$ is obtained at a slightly higher PDA temperature $T_{\text{an}} = 940 \text{ }^\circ\text{C}$. On the account of P_{b0} , it appears that for annealing from $T_{\text{an}} > 900 \text{ }^\circ\text{C}$ onward, the interface starts to break up first, where it is interesting to note that, in the range $T_{\text{an}} \sim 900\text{--}940 \text{ }^\circ\text{C}$, the *EX* density still increases while the P_{b0} density already starts to decrease. So, the overall picture emerging from the curves in Fig. 2 is that, as compared to P_{b0} , the manifestation of the *EX* peak is delayed in terms of T_{an} . The true character of the Si/SiO_x-type interface is disrupted first (elimination of interfacial Si-dangling bonds), but for $T_{\text{an}} \geq 940 \text{ }^\circ\text{C}$, the defects rapidly disappear altogether, pointing to drastic disintegration of the interfacial region, i.e., elimination of the “pure” SiO_x component. For clarity, this disappearance of the ESR-active centers is not due to inadvertent H passivation, as verified by applying additional vuv irradiation after some PDA steps.

It is interesting to put the acquired atomic level information in terms of occurring point defects in the perspective of previous morphological/compositional studies on the Si/LaAlO₃ structure. Recent work¹⁵ has investigated the thermal stability of (100)Si/LaAlO₃/Al₂O₃ stacks against RTA in N₂ ambient at 850–1040 °C for 10–20 s. As observed by atomic force microscopy and x-ray diffraction, the work reports that RTA from 900 °C onward starts to induce changes in surface morphology, together with initiation of the transformation of the amorphous to polycrystalline state. Secondary-ion-mass spectroscopy profiling shows substantial penetration of Al and La atoms into the Si substrate for RTA at or above 950 °C, and the penetration remains below the detection limit for $T_{\text{an}} \leq 935 \text{ }^\circ\text{C}$. Our ESR data may well fit within this morphological picture: In terms of T_{an} , we may link the initiation of the formation of a Si/SiO_x-type interface with the very early onset of LaAlO₃ film crystallization, followed by some more substantial SiO_x-type interlayer growth with increasing T_{an} . For clarity, though, the appearance of the P_{b0} centers cannot be directly linked to the grain boundary regions per se, as this would conflict with the observed ESR spectral anisotropy in registry with the crystalline (100) Si surface. Then, for T_{an} further increasing above $\sim 940 \text{ }^\circ\text{C}$, the progressing interdiffusion chemically destroys the pristine nature of the SiO_x component (possibly silicate formation) resulting in the obliteration of the SiO_{2(v)}-specific point defects. It is possible that the onset temperature for La and Al outdiffusion in the current case is somewhat lower considering the applied longer PDA treatment times (10 min) as compared to previous RTA work (10–20 s).

Also, within the interpretation, it appears we detect the initiation of crystallization of the a-LaAlO₃ film somewhat at lower T_{an} than in previous work.¹⁶ Again, this may partly have resulted from the applied longer anneal times in conjunction with the presence of O₂ in the anneal ambient. Yet, it may as well bear out that ESR is prone to detect interfacial

reshaping in a very embryotic state, ahead of standard morphological/compositional methods.

In summary, ESR has been successfully applied to assess the nature of the interface in (100)Si/LaAlO₃ entities and thermally induced alterations. It is found that the (100)Si/LaAlO₃ structure exhibits a high quality and robust interface in terms of dangling-bond-type interface defects. This interface appears to be stable under extended thermal anneals up to $\sim 850 \text{ }^\circ\text{C}$, suggesting the possibility of nearly perfect matching of the Si crystal lattice and the LaAlO₃ network. Upon annealing at $T_{\text{an}} \geq 860 \text{ }^\circ\text{C}$ a SiO_x-type interlayer is formed as evidenced by the appearance of P_{b0} interface defects, likely indicating the onset of crystallization of the a-LaAlO₃ film. At somewhat higher T_{an} , the *EX* defect is observed. The delay in appearance of *EX* vis-à-vis P_{b0} points to additional growth of the SiO_x-type interlayer. Upon annealing at $T_{\text{an}} \geq 930 \text{ }^\circ\text{C}$, however, the Si/SiO_x-nature of the interlayer starts to break up, resulting in fast, likely compositional, transformation with increasing T_{an} as signaled by the disappearance of the SiO_x related defects altogether. It could be related to the diffusion of La and Al into the silicon substrate and possibly formation of a silicate interlayer.

Two of the authors (L.F.E. and D.G.S.) gratefully acknowledge the financial support of the Semiconductor Research Corporation (SRC) and SEMATECH through the SRC/SEMATECH FEP Center. Another author (L.F.E.) gratefully acknowledges an AMD/SRC fellowship.

¹International Technology Roadmap for Semiconductors (Semiconductor Industry Association, San Jose, CA, 2005).

²G. D. Wilk, R. M. Wallace, and J. M. Anthony, *J. Appl. Phys.* **89**, 5243 (2001).

³M. A. Quevedo-Lopez, M. El-Bouanani, B. E. Gnade, R. M. Wallace, M. R. Visokay, M. Douglas, M. J. Bevan, and L. Colombo, *J. Appl. Phys.* **92**, 3540 (2002).

⁴J. Robertson, *Eur. Phys. J.: Appl. Phys.* **28**, 265 (2004).

⁵See, e.g., W. Vandervorst, B. Brijs, H. Bender, O. T. Conrad, J. Petry, O. Richard, S. Van Elshocht, A. Delabie, M. Caymax, and S. DeGendt, *Mater. Res. Soc. Symp. Proc.* **745**, 23 (2003).

⁶A. Stesmans and V. V. Afanas'ev, *J. Phys.: Condens. Matter* **13**, L673 (2001); *Appl. Phys. Lett.* **80**, 1957 (2002).

⁷J. L. Cantin and H. J. von Bardeleben, *J. Non-Cryst. Solids* **303**, 175 (2002); S. Baldovino, S. Nokrin, G. Scarel, M. Fanciulli, T. Graf, and M. S. Brandt, *ibid.* **322**, 168 (2003); A. Y. Kang, P. M. Lenahan, J. F. Conley, Jr., and R. Solanski, *Appl. Phys. Lett.* **81**, 1128 (2002).

⁸R. Helms and E. H. Poindexter, *Rep. Prog. Phys.* **57**, 791 (1994).

⁹K. Brower, *Phys. Rev. B* **33**, 4471 (1986).

¹⁰A. Stesmans, *Phys. Rev. B* **48**, 2418 (1993).

¹¹A. Stesmans, B. Nouwen, and V. V. Afanas'ev, *Phys. Rev. B* **58**, 15801 (1998).

¹²A. Stesmans and V. V. Afanas'ev, *J. Appl. Phys.* **83**, 2449 (1998).

¹³B. E. Park and H. Ishiwara, *Appl. Phys. Lett.* **79**, 806 (2001).

¹⁴L. F. Edge, D. G. Schlom, R. T. Brewer, Y. J. Chabal, J. R. Williams, S. A. Chambers, C. Hinkle, G. Lucovsky, Y. Yang, S. Stemmer, M. Copel, B. Holländer, and J. Schubert, *Appl. Phys. Lett.* **84**, 4629 (2004).

¹⁵P. Sivasubramani, M. J. Kim, B. E. Gnade, R. M. Wallace, L. F. Edge, D. L. Schlom, H. S. Craft, and J. P. Maria, *Appl. Phys. Lett.* **86**, 201901 (2005).

¹⁶A. Stesmans, *Phys. Rev. B* **45**, 9501 (1992); A. Stesmans and F. Scheerlinck, *ibid.* **50**, 5204 (1994); *J. Appl. Phys.* **75**, 1047 (1994).

¹⁷A. Baumer, M. Stutzmann, M. S. Brandt, F. C. K. Au, and S. T. Lee, *Appl. Phys. Lett.* **85**, 943 (2004); W. E. Carlos and S. M. Prokes, *J. Appl. Phys.* **78**, 2129 (1995); M. Dohi, H. Yamatani, and T. Fujita, *ibid.* **91**, 815 (2002).

¹⁸W. Futako, T. Umeda, M. Nishizawa, T. Yasuda, J. Isoya, and S. Yamasaki, *J. Non-Cryst. Solids* **299-302**, 575 (2002).

¹⁹A. Stesmans and V. V. Afanas'ev, *J. Appl. Phys.* **97**, 033510 (2004).